Thermodynamics of thermally-driven adsorption compression

Thermodynamics of thermally-driven adsorption compression

Giulio Santori[a]*, Mauro Luberti[a]
*corresponding author: Dr. Giulio Santori, g.santori@ed.ac.uk, tel: +4401316519043, fax: +4401316506551
[a] The University of Edinburgh, School of Engineering, Institute for Materials and Processes, Sanderson Building, The King's Buildings, Mayfield Road, EH9 3JL, Edinburgh, Scotland, UK

Abstract
Adsorption compressors are an emerging technology used to compress a gas stream with low grade heat which is of interest for the next long term extra-planetary bases. An analysis of thermodynamics of multicomponent gas/vapour mixtures compression with a thermally-driven adsorption bed is reported. In this unit a multicomponent stream is firstly adsorbed and secondly compressed by heating a bed at closed volume. The analysis is based on adsorbed solution theory applied to closed vessels where the composition and pressure of the bulk gas phase depends on temperature and volume of the whole system, leading to an isochoric-isothermal flash problem. Analysis of both an ideal and non-ideal adsorption compressor shows that the ideal approach is conservative, resulting in lower compression ratios at higher energy consumption.

Keywords: Isothermal flash; Isochoric flash; Adsorbed solution theory; Common tangent plane; Solid compressor; Adsorption compressor; Adsorption thermodynamics;

1. Introduction

The recent development of highly selective adsorption materials have enabled their integration in a number of traditional technologies, resulting in advanced processes demanding a sensibly lower energy consumption delivered at lower temperatures than their traditional counterparts [1-3]. A partial list of cases is included in Table 1. All these new technologies include a fundamental component that is the adsorption bed, which can be structured in numerous different shapes depending on the regeneration strategy [4-7].

Table 1: Emerging adsorption technologies

Sector	Traditional technology	Adsorptive technology	Ref.
Refrigeration & air conditioning	Electrically-driven vapour compression system	Adsorption refrigerators & heat pumps	[8-10]
Drying	Electrical dishwasher	Adsorption dishwasher	[11]
Desalination	Multi-effect distillation	Adsorption desalination	[12]
CO_2 removal	Absorption	Temperature and/or vacuum swing adsorption	[13-15]

Adsorption beds are often operated as open systems where a single or multicomponent feed flows through the unit. However, some emerging technologies need to operate adsorption beds as closed systems. This is the case of the carbon dioxide removal and compression system, currently operating on the International Space Station and still under development to serve the next long term Mars or lunar bases [16-18].
Adsorption is the favourite method to produce a compressed gas in space applications because it does not have moving parts, requiring virtually no maintenance, and does not generate vibrations. The carbon dioxide removal system is the upstream process of the Sabatier reaction, which will be used in extra-terrestrial bases for the production of water. As demonstrated elsewhere [19, 20], the standard operating conditions to drive the Sabatier reaction towards higher CO_2 conversion are temperature ranging between 250-400°C and pressure of reagents greater than 130 kPa. So, compression of CO_2 from 20 kPa (Mars atmosphere) to 130 kPa (Sabatier reaction pressure) is required, resulting in a minimum compression ratio of 6.5.
In this technology, compression is performed through a change in the bed temperature at closed volume. The operational steps of an adsorption compressor can be scheduled as:
1) Adsorption step: the adsorption bed is kept isothermal and is fed with the inlet stream at constant pressure and temperature.
2) Heating step: the bed is heated at constant volume. The new equilibrium state after heating results in a partition of the components between bulk gas phase and adsorbed phase at a bulk gas phase pressure higher than the initial pressure during the feeding. The pressure increase is mainly because of the release of material from the adsorbed phase to the bulk gas phase. The composition and the level of pressure in the bulk gas phase depend on the final temperature, volume available for the bulk gas phase, mass of adsorbent and total amount of moles in the enclosure.

3) Supply step: the outlet valve is open with a decrease in pressure and a variable flow of material is discharged.

Thus, adsorption compressors are thermally-driven compression systems adopting adsorption materials and operating according to temperature swing adsorption processes. An early thermodynamic analysis for adsorption of pure fluids has been presented in [21, 22] but no thermodynamic basis has been provided for the adsorption compression of a multicomponent mixture to date and some units such as the air revitalization module of the International Space Station (ISS) have been designed on the basis of simplifying assumptions, refining the performance in successive, trial and error steps. The air revitalization unit of the ISS uses zeolites 5A and 13X which adsorb significant amounts of carbon dioxide and nitrogen. This aspect has been addressed, at the design stage, by oversizing the mass of required material with a safety factor [22, 23]. The present work provides a tool for consistent thermodynamic investigation of adsorption compression of multicomponent gas mixtures.

The fundamental calculation for adsorption compression is the isochoric-isothermal flash (VT flash). VT flash in bulk gas/adsorbed phase equilibria has been already formulated by minimization of the Helmholtz energy of the system [24]. In this work we show that the well-known Rachford-Rice system of equations can be also applied to adsorption equilibrium after appropriate modifications.

For sake of clarity, at first an ideal ternary mixture in equilibrium with an ideal adsorbed solution [25] is evaluated. The aim is to provide the thermodynamic framework for the simple ideal case. Secondly, a non-ideal ternary mixture is considered using the Soave-Redlich-Kwong (SRK) equation of state for the description of the bulk gas phase and a Gibbs excess model for the adsorbed phase. This is aimed to show the differences between an ideal and non-ideal formulation.

Since no experimental multicomponent equilibrium data are presently available for this problem, the thermodynamic consistency of the results is validated through the common tangent plane approach for adsorption derived in [26]. The last section of this work is devoted to the performance analysis of ideal and non-ideal compressors.

2. Ideal isothermal-isochoric flash for adsorption

The ideal case includes an ideal bulk gas phase in equilibrium with an ideal adsorbed solution. The pressure and compositions in the new equilibrium state can be calculated considering the usual method based on the Rachford-Rice equations system [27], once a number of additional conditions arising from the adsorbed solution theory are provided [28]. The resulting system of equations for NC components is:

$$\sum_{i}^{NC} \frac{z_i\left(k_i-1\right)}{1+\frac{G}{F}\left(k_i-1\right)}=0 \tag{1}$$

$$x_i=\frac{z_i}{1+\frac{G}{F}\left(k_i-1\right)} \tag{2}$$

$$G=\frac{P_{bulk}V_{void}}{RT} \tag{3}$$

$$k_i=\frac{P_i^0}{P_{bulk}} \tag{4}$$

$$y_iP_{bulk}=P_i^0x_i \tag{5}$$

$$\frac{m_{ads}}{N}=\sum_{i=1}^{NC}\left(\frac{x_i}{n_i}\right) \tag{6}$$

$$\psi_i=\int_0^{P_i^0} n_i\, d\left(\ln P_i\right) \qquad i=1,2,....NC \tag{7}$$

$$\psi_i=\psi_{eq} \qquad i=1,2,....NC \tag{8}$$

$$F-\left(G+N\right)=0 \tag{9}$$

Eq. (1) is the original Rachford-Rice solving equation; eq. (3) is the ideal gas equation of state for the calculation of the amount of moles in the bulk gas phase. Eqns (4-8) follow the ideal adsorbed solution

theory [27, 28]. Eq. (9) is the overall mass balance. Assuming that the adsorbent occupies all the volume available in the vessel, the gas mixture volume is calculated by:

$$V_{void} = \frac{m_{ads}}{\rho_b}\left(\varepsilon_b + \left(1-\varepsilon_b\right)\varepsilon_p\right) \tag{10}$$

Usually the parameters involved in eq. (10) are omitted in equilibrium measurements. This work assumes the values reported in Table 2. Although the values of Table 2 do not perfectly correspond to the experimental equilibrium data used for single isotherm parameters regression, they lay in the average range commonly assumed for this kind of materials.

The system of eqns (1-9) can be reduced in a straightforward way to only two equations by substitution of variables, holding the final variables P_{bulk} and reduced grand potential ψ_{eq}. The equivalent two equation system includes eq. (1) and eq. (9).

Table 2: Adsorption materials and beds properties

	m_{ads} [kg]	ε_b	ε_p	ρ_b [kg m^{-3}]	Ref
Zeolite 5A	1	0.39	0.50	687	[29]
Activated Carbon Norit R1 Extra	1	0.35	0.84	420	[30]
Zeolite 13X	1	0.37	0.60	641	[31]

Eqns (1-9) can be effectively solved by the Newton numerical method without any issue on the estimation of the best initial guess. That is because the system has always only one solution in the physically meaningful domain $P_{bulk}>0$ and $\psi_{eq}>0$. In order to show this feature for the ideal problem, the Nitrogen/Oxygen/Argon ternary system adsorption on zeolite 5A has been considered, using the Langmuir isotherm with parameters reported in Table 3.

Table 3: Parameters of the Langmuir isotherm model for Nitrogen, Oxygen and Argon on zeolite 5A at 298.55 K. Equilibrium data are from [32].

	Pressure Range [kPa]	q_s [mol kg^{-1}]	b [kPa^{-1}]
N_2 (1)	34.1-442.9	2.114	0.001756
O_2 (2)	29.3-404.8	2.313	0.000524
Ar (3)	35.5-438.7	3.348	0.000314

Fig. 1 illustrates the solution of the system composed by eq. (1) and eq. (9). In the physically meaningful region, the two functions intersect only in one point. The same equilibrium compositions are confirmed by the common tangent plane of Gibbs energy of mixing (Fig. 2). The presence of a common tangent plane of the Gibbs energy of mixing at the equilibrium point of Table 4 validates the thermodynamic consistency of the solution. In Table 4 it can be noted that while the bulk gas phase composition is very different from the feed, being enriched by oxygen and argon which are the less strongly adsorbed components, the adsorbed phase composition is close to the feed, being slightly richer in nitrogen over the other components.

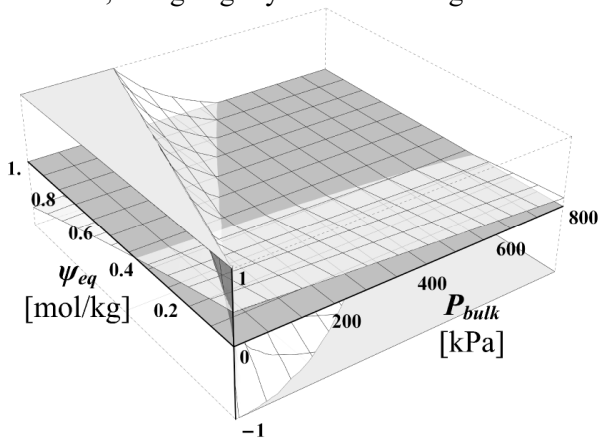

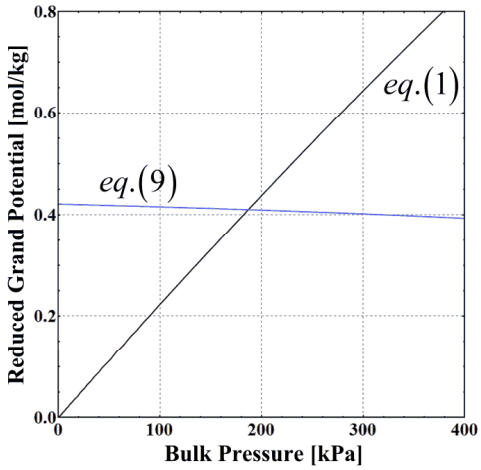

Figure 1: Surfaces representing the left hand side functions of eq. (1) and eq. (9) (top). The horizontal plane passing through (0, 0, 0) defines the contour curves corresponding to eq. (1) and eq. (9) (bottom). eq. (1) and eq. (9) intersect in only one point, highlighting that the solution is necessary and sufficient.

Table 4: Solution for the ideal VT flash calculation at the conditions: V_{void} = 1.021 10^{-3} m^3; F = 0.45 moles; T = 298.55 K

Component	z_i	P_{bulk} [kPa]	ψ_{eq} [mol kg^{-1}]	x_i	P_i^0 [kPa]	y_i
N_2 (1)	0.70	186.80	0.410	0.744	122.03	0.486
O_2 (2)	0.25			0.214	370.54	0.425
Ar (3)	0.05			0.042	398.20	0.089

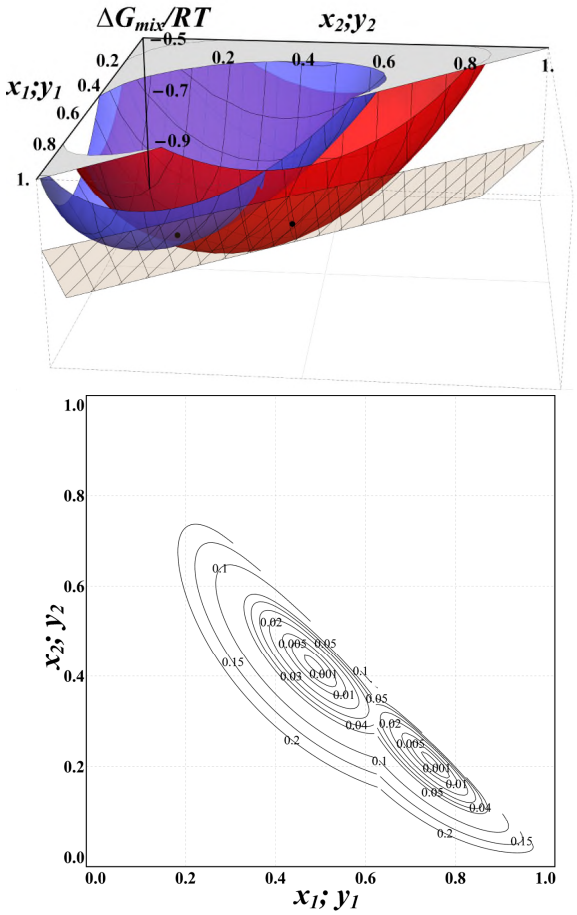

Figure 2: Common tangent plane of the Gibbs energy of mixing at the equilibrium point of Table 4 (top). Contour plot of the distance function between Gibbs energy of mixing and common tangent plane at the equilibrium point of Table 4 (bottom).

3. The non-ideal isothermal-isochoric flash

In the non-ideal formulation fugacity and activity coefficients respectively for the bulk gas phase and the adsorbed phase are considered [33]. Based on the experimental measurement reported in [34], the ternary mixture Methane/Nitrogen/Carbon Dioxide on activated carbon Norit R1 Extra at 298 K and high pressure is analysed. Single component adsorption experimental data were fitted using the Unilan isotherms, considering the absolute adsorbed amount versus fugacity, resulting in the parameters of Table 5.

Table 5: Parameters of the Unilan isotherm model for Methane, Nitrogen and Carbon Dioxide on activated carbon Norit R1 Extra at 298 K. Experimental data are from [34].

	Pressure Range [kPa]	Fugacity Range [kPa]	q_s [mol kg^{-1}]	b [kPa^{-1}]	s
CH_4 (1)	0-5753	0-5219	24.537	2.873 10^{-5}	5.220
N_2 (2)	0-5958	0-5934	21.187	1.403 10^{-5}	4.759
CO_2 (3)	0-6000	0-4239	34.824	5.833 10^{-5}	5.086

3.1 Bulk gas phase model

The eqns (3-7) must be modified introducing fugacity for the description of the bulk gas phase and activity coefficients for the adsorbed phase. The SRK [35, 36] equation of state has been used for the evaluation of the fugacity coefficients.

$$Z^3 - Z^2 + Z\left(A - B - B^2\right) - AB = 0 \tag{11}$$

$$\ln\left(\varphi_{i,bulk}\right) = \frac{b_i}{b}\left(Z-1\right) - \ln\left(Z-B\right) - \frac{A}{B}\left(2\frac{a_i^{1/2}}{a^{1/2}} - \frac{b_i}{b}\right)\ln\left(1+\frac{B}{Z}\right) \tag{12}$$

Eq. (11) is the fugacity coefficient of component i in the bulk gas phase from SRK equation of state. The correlations for the calculation of the parameters of eq. (11) and (12) are reported elsewhere [37]. The interaction parameters are neglected in all of the following calculations and the number of total moles of the mixture in the bulk phase (G) is derived by the compressibility factor Z as follows:

$$G = Z\frac{P_{bulk}V_{void}}{RT} \tag{13}$$

3.2 Excess Gibbs energy model for the adsorbed phase

The adopted activity coefficient model is the ABC equation [38]. At constant temperature, it proposes the following expression for the excess Gibbs energy:

$$g_{ex} = \sum_{i=1}^{NC}\sum_{i>j\ j=1}^{NC} A_{0,ij}\,x_i x_j\left(1 - e^{-C_{ij}\psi}\right) \tag{14}$$

Its application requires the preliminary regression on the experimental data of binary systems of the binary interaction parameters $A_{0,ij}$ and C_{ij} at constant temperature. The results of the regression on the binary experimental data in [34] are reported in Table 6.

Table 6: Parameters of the ABC equation for Methane, Nitrogen and Carbon Dioxide binary systems on activated carbon Norit R1 Extra at 298 K. Experimental data are from [34].

Components (i/j)	Fugacity range [kPa]	$A_{0,ij}$ [kJ mol^{-1}]	C_{ij} [kg mol^{-1}]
CH_4/N_2 (1/2)	150.9-5578.7	−1.726	10.060
CH_4/CO_2 (1/3)	97.7-5342.1	0.474	0.0162
N_2/CO_2 (2/3)	107.9-4459.2	1.017	14.699

The activity coefficients are defined as:

$$RT\ln\left(\gamma_i\right) = \left.\frac{\partial\left(Ng_{ex}\right)}{\partial n_i}\right|_{T,\psi,n_j} \tag{15}$$

where N is the total amount of moles adsorbed. According to the definition of eq. (15), for a ternary system, the activity coefficients result in:

$$\ln(\gamma_1)=\frac{\left(e^{-(C_{12}+C_{13}+C_{23})\psi}\right)}{RT\left(x_1+x_2+x_3\right)^2}\left(\begin{array}{l}A_{0,12}e^{(C_{13}+C_{23})\psi}\left(e^{C_{12}\psi}-1\right)x_2\left(x_2+x_3\right)+\\ +A_{0,23}\left(e^{(C_{12}+C_{13})\psi}-e^{(C_{12}+C_{13}+C_{23})\psi}\right)x_2x_3+\\ +A_{0,13}e^{(C_{12}+C_{23})\psi}\left(e^{C_{13}\psi}-1\right)\left(x_2+x_3\right)x_3\end{array}\right) \tag{16}$$

$$\ln(\gamma_2)=\frac{\left(e^{-(C_{12}+C_{13}+C_{23})\psi}\right)}{RT\left(x_1+x_2+x_3\right)^2}\left(\begin{array}{l}A_{0,12}e^{(C_{13}+C_{23})\psi}\left(e^{C_{12}\psi}-1\right)x_1\left(x_1+x_3\right)+\\ +A_{0,13}\left(e^{(C_{12}+C_{23})\psi}-e^{(C_{12}+C_{13}+C_{23})\psi}\right)x_1x_3+\\ +A_{0,23}e^{(C_{12}+C_{23})\psi}\left(e^{C_{23}\psi}-1\right)\left(x_1+x_3\right)x_3\end{array}\right) \tag{17}$$

$$\ln(\gamma_3)=\frac{\left(e^{-(C_{12}+C_{13}+C_{23})\psi}\right)}{RT\left(x_1+x_2+x_3\right)^2}\left(\begin{array}{l}A_{0,13}e^{(C_{13}+C_{23})\psi}\left(e^{C_{13}\psi}-1\right)x_1\left(x_1+x_2\right)+\\ +A_{0,12}\left(e^{(C_{13}+C_{23})\psi}-e^{(C_{12}+C_{13}+C_{23})\psi}\right)x_1x_2+\\ +A_{0,23}e^{(C_{12}+C_{13})\psi}\left(e^{C_{23}\psi}-1\right)\left(x_1+x_2\right)x_2\end{array}\right) \tag{18}$$

To take into account the non-idealities both in adsorbed and bulk gas phase, eqns. (6) and (7) are now replaced by eqns (19) and (20):

$$\psi_i=\int_0^{f_{i,ads}} n_i\,d\left(\ln f_i\right)\qquad i=1,2,....NC \tag{19}$$

Eq. (19) is an integral function of each single isotherm. In the ideal case it is fitted directly on the experimental pressures, in the non-ideal the isotherms have to be fitted on the fugacity, modifying the experimental pressure with an equation of state (in this case SRK).

$$\frac{m_{ads}}{N}=ex+\sum_{i=1}^{NC}\frac{x_i}{n_i} \tag{20}$$

where the excess contribution to the total number of adsorbed moles *ex* is given by:

$$ex=\left.\frac{\partial\left(g_{ex}/RT\right)}{\partial\psi}\right|_{T,x}=\sum_{i=1}^{NC}\sum_{i>j}^{NC}\sum_{j=1}\left(\frac{A_{0,ij}C_{ij}}{RT}x_ix_je^{-C_{ij}\psi}\right) \tag{21}$$

The two contributions on the right hand side of eq. (20) are respectively the contribution of the non-idealities in the adsorbed phase according to the ABC equation and the contribution considering ideal adsorption of a non-ideal gas mixture. In fact, in eq. (20), n_i is the adsorption isotherm of the pure component i with parameters regressed on fugacities instead of pressures [28].

3.3. Non-ideal flash calculation

The k_i factors for the non-ideal case are no longer only function of pressures but also of the compositions because of the presence of the fugacity coefficient in the bulk gas phase ($\varphi_{i,bulk}$), the activity coefficient of the adsorbed phase (γ_i) and the fugacity of the pure component i in adsorbed phase ($f_{i,ads}$). Therefore k_i factors become:

$$\frac{y_i}{x_i}=\frac{f_{i,ads}\gamma_i}{\varphi_{i,bulk}P_{bulk}} \tag{22}$$

This feature makes the system of equations larger and more nonlinear than the ideal case. Furthermore, in order to have consistency between the number of equations and the number of variables, for a three components mixture, three isofugacity condition equations and conservation of moles equation for one of the components must be included.

The Newton method can again effectively solve this problem, providing an initial guess reasonably close to the actual solution, e.g. assuming a value of 1 for fugacity and activity coefficients. After some sensitivity analysis, it has been noticed that the convergence to a feasible solution is affected by the initial value of P_{bulk} more than the initial value of the other variables.

Assuming the parameters of Tables 5 and 6, the results of the calculation for the non-ideal high pressure case are reported in Table 7. Carbon dioxide, being the most strongly adsorbed component, exhibits a higher

concentration in the adsorbed phase compared to the feed; an opposite trend can be seen for methane and nitrogen components. The result is again validated testing the presence of the common tangent plane of the Gibbs energy of mixing surface at the equilibrium (Fig. 3).

Table 7: Solution for the non-ideal VT flash calculation at the conditions: V_{void} = 2.133 10^{-3} m^3; F = 10 moles; T = 298 K

Component	z_i	P_{bulk} [kPa]	ψ_{eq} [kg/mol]	x_i	γ_i	$f_{i,ads}$ [kPa]	y_i	$\varphi_{i,bulk}$
CH_4 (1)	0.4	2837.29	14.336	0.373	0.980	3784.88	0.511	0.511
N_2 (2)	0.1			0.052	0.970	13724.31	0.239	0.239
CO_2 (3)	0.5			0.575	1.029	1055.05	0.250	0.250

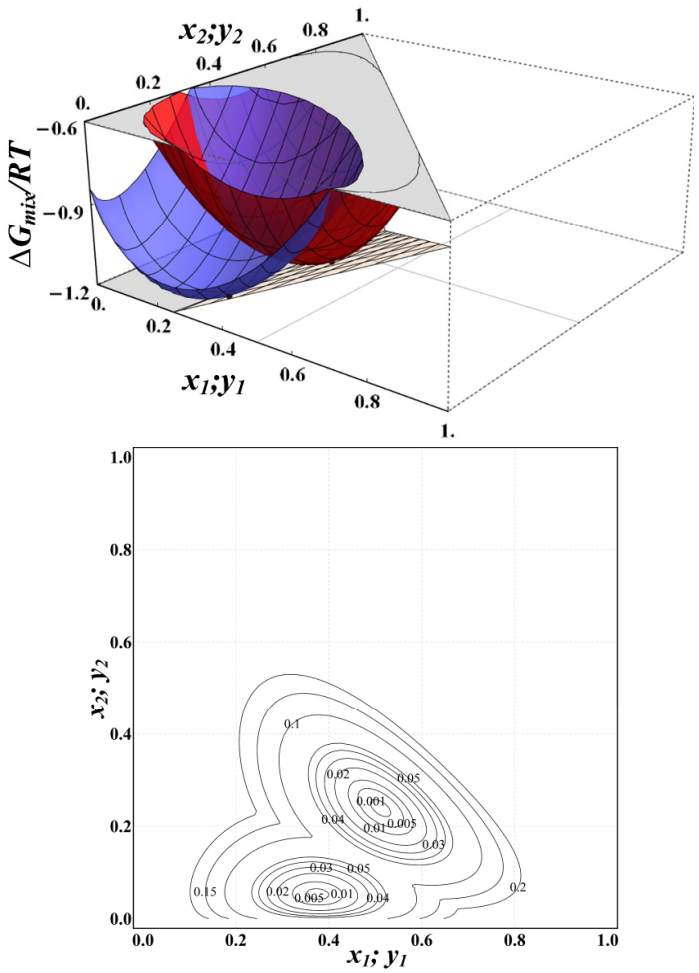

Figure 3: Common tangent plane of the Gibbs energy of mixing locating at the equilibrium point calculated in Table 7 (top). Contour plot of the distance function between Gibbs energy of mixing and common tangent plane at the equilibrium point of Table 7 (bottom).

4. Enthalpy of adsorption

The thermal energy required for compression includes both enthalpy of desorption and sensible heat. In case of multicomponent mixture, the enthalpy of desorption ΔH_{ads} [kJ] can be calculated following the derivation described in [38]:

$$\Delta H_{ads} = m_{ads} \sum_{i=1}^{NC} \left(\int_0^{n_i^o} \Delta \bar{h}_i \, dn_i \right) \tag{23}$$

where $\Delta \bar{h}_i$ is the differential enthalpy of adsorption [kJ mol^{-1}] of the i^{th} component of the mixture. For non-ideal adsorbed solutions and non-ideal bulk gases, the differential enthalpy is:

$$\Delta\bar{h}_i = \Delta h_i^o + RT^2\left(\frac{\partial \ln \gamma_i}{\partial T}\right)_{\psi,x} + \left[\frac{1}{n_i^o} + \left(\frac{\partial \ln \gamma_i}{\partial \psi}\right)_{T,x}\right]$$

$$\times\left[\frac{\sum_j x_j G_j^o n_j^o\left(\Delta\bar{h}_j^o - \Delta h_j^o\right) + RT^2\left(\frac{\partial(ex)}{\partial T}\right)_{\psi,x}}{\sum_j x_j G_j^o - \left(\frac{\partial(ex)}{\partial T}\right)_{T,x}}\right] \qquad \text{i=1,2,…NC} \qquad (24)$$

which, for an ideal gas adsorbed ideally, becomes:

$$\Delta\bar{h}_i = \Delta h_i^o + \frac{1}{n_i^o}\left(\frac{\sum_j x_j G_j^o n_j^o\left(\Delta\bar{h}_j^o - \Delta h_j^o\right)}{\sum_j x_j G_j^o}\right) \qquad \text{i=1,2,…NC} \qquad (25)$$

The terms composing eq. (24) are:

$$G_i^o = \frac{1}{\left(n_i^o\right)^2}\left(\frac{\partial \ln n_i^o}{\partial \ln f_i}\right)_T \qquad \text{i=1,2,…NC} \qquad (26)$$

Eq. (24) is a function of the pure component molar integral enthalpy of adsorption [kJ mol^{-1}], which neglecting the Poynting term, becomes:

$$\Delta h_i^o = \frac{1}{n_i^o} T^2 \frac{\partial}{\partial T}\left(\frac{\Omega_i}{T}\right)_{f_i} \qquad (27)$$

where Ω [kJ kg^{-1}] is the grand potential of adsorption. The other variable in eq. (24) is the pure component differential enthalpy [kJ mol^{-1}]:

$$\Delta\bar{h}_i^o = RT^2\left(\frac{\partial \ln f_i}{\partial T}\right)_{n_i} \qquad (28)$$

Assuming that the specific heats of the gases are constant in the operating range of temperatures and the specific heats in adsorbed and bulk gas phase are identical [39], the sensible heat can be derived as follows:

$$\Delta H_{sens} = \left[m_{ads} c_{p,ads} + \sum_i^{NC}\left(n_{i,bulk} + n_{i,ads}\right) c_{p,i}\right]\left(T_{heating} - T_{ads}\right) \qquad (29)$$

where $c_{p,ads}$ is the specific heat capacity of the adsorbent assumed 0.858 kJ kg^{-1} K^{-1} [11], $c_{p,i}$ is the bulk gas phase specific heat capacity of the i^{th} component of the mixture [kJ mol^{-1} K^{-1}] as reported in [40]. $n_{i,bulk}$ is the number of moles of component i in the bulk gas phase [mol] and $n_{i,ads}$ is the number of moles of component i in the adsorbed phase [mol], T_{ads} is the adsorption temperature which is kept at 298 K and $T_{heating}$ is the heating temperature.

5. Ideal adsorption compression

The case of a solid compressor is presented where 1 kg of zeolite 13X adsorbs from a three components feed mixture of Nitrogen, Oxygen, Carbon Dioxide with composition (0.7897,0.2099, 0.0004) mole fraction at 101.325 kPa, 298 K in accordance to the ideal adsorbed solution theory, with adsorption isotherms parameters reported in Table 8.

Table 8: Langmuir, Dual Site Langmuir and Toth isotherm parameters of the ideal and non-ideal adsorption zeolite 13X compressor

	Isotherm	q_{s1} [mol/kg]	b_{01} [kPa^{-1}]	ΔH_1 [kJ mol^{-1}]	q_{s2} [mol kg^{-1}]	b_{02} [kPa^{-1}]	ΔH_2 [kJ mol^{-1}]	t	Ref
N_2	Langmuir	4.725	$3.616\ 10^{-7}$	−19.59	--	--	--	--	[41]
O_2	Langmuir	4.650	$1.452\ 10^{-5}$	−7.80	--	--	--	--	[41]
CO_2	Dual site Langmuir	3.573	$1.681\ 10^{-8}$	−35.00	1.789	$3.812\ 10^{-9}$	−49.26	--	[42]
C_2H_4	Toth	2.21	$5.22\ 10^{-6}$	−21.4	--	--	--	1.75	[43]
C_2H_6	Toth	2.72	$1.13\ 10^{-7}$	−36.3	--	--	--	0.97	[43]

After adsorption, the bed is heated up at closed volume. The significant amount of material moving from the adsorbed phase to the bulk gas phase causes a pressure increase with a magnitude depending on the heating temperature (Fig. 4).

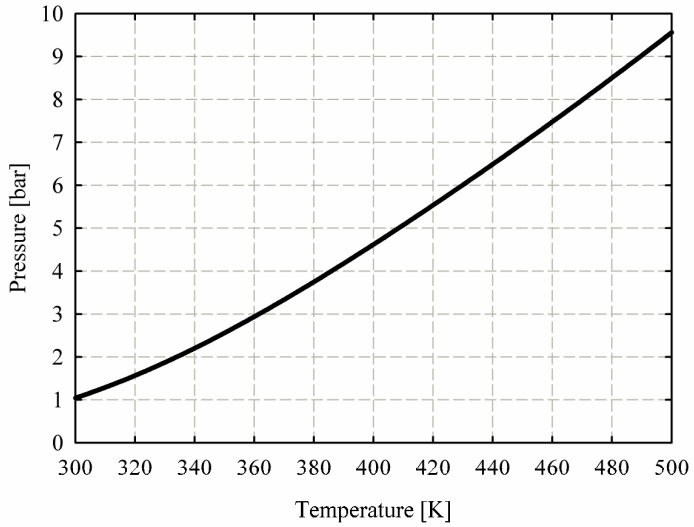

Figure 4: Evolution of the bulk gas phase pressure heating the bed at different temperature levels for 1 kg of zeolite 13X compressing a stream of Nitrogen, Oxygen, Carbon Dioxide adsorbed at 101.325 kPa, 298 K and composition (0.7897, 0.2099, 0.0004) mole fraction.

The composition of the compressed stream is variable because of the changed temperatures and bulk gas phase pressures. Fig. 5 highlights the change in bulk gas phase composition along with the increase in the amount of gas mixture n_{bulk} when the adsorption bed is heated.

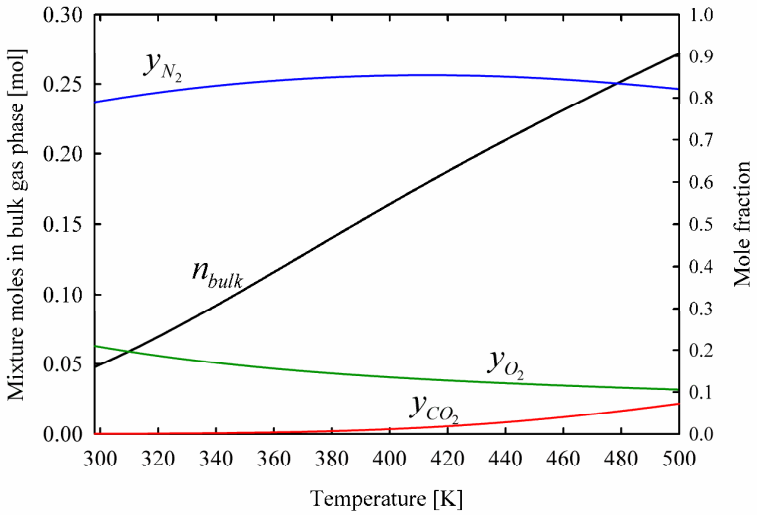

Figure 5: Evolution of the gas mixture moles (left) and component mole fraction (right) at different heating temperatures for 1 kg of zeolite 13X compressing a stream of Nitrogen, Oxygen, Carbon Dioxide adsorbed at 101.325 kPa, 298 K and composition (0.7897, 0.2099, 0.0004) mole fraction.

Fig. 6 shows that the dominant part in the total energy required for compression is the sensible heat, accounting, in this particular case, for an average of 91% of the total energy.

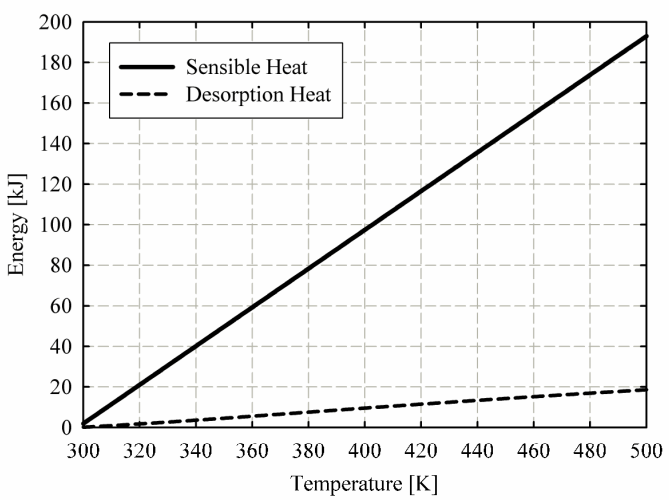

Figure 6: Evolution of sensible and desorption heat at different heating temperatures for 1 kg of zeolite 13X compressing a stream of Nitrogen, Oxygen, Carbon Dioxide adsorbed at 101.325 kPa, 298 K and composition (0.7897, 0.2099, 0.0004) mole fraction

6. Non-ideal adsorption compression

When adsorption cannot be described as ideal, ideal and non-ideal interpretations can results in significant performance discrepancies. In this section a gas mixture of Carbon Dioxide/Ethylene/Ethane adsorbed on zeolite 13X is considered. This gas mixture shows non-ideal behaviour in gas phase already at moderate pressure and ambient temperature and non-idealities in adsorbed phase on zeolite 13X. As measured in [30 38], ABC equation excess model can describe correctly the equilibrium of a non-ideal adsorbed phase of Carbon Dioxide/Ethylene/Ethane on zeolite 13X with the binary interaction parameters of Table 9. The bulk gas phase, especially for Ethane and Ethylene, require the specification of an equation of state for the calculation of fugacity coefficient in the range of operating conditions. Accordingly SRK equation of state is used to describe the thermodynamic behaviour of the bulk gas phase.

Table 9: Parameters of the ABC equation for Carbon Dioxide, Ethylene and Ethane binary systems on zeolite 13X. Experimental data are from [38].

Components (i/j)	A_{ij} [kJ mol^{-1}]	B_{ij} [kJ mol^{-1} K^{-1}]	C_{ij} [kg mol^{-1}]
CO_2/C_2H_6 (1/3)	-10.0	0.01917	0.110
CO_2/C_2H_4 (1/2)	-6.5	0.01450	0.030
C_2H_4/C_2H_6 (2/3)	-4.5	0.00437	0.067

Note: temperature dependent interaction parameters are considered according to $A_{0,ij} = A_{ij} + T B_{ij}$

In the first operational step, the adsorption compressor is loaded at 101.325 kPa and 298 K with a multicomponent gas mixture having composition (0.05, 0.15, 0.8) mole fraction. Table 10 reports the distribution of the components in bulk gas phase and adsorbed phase at this initial adsorption step. The non-ideal approach predicts more amount of initial gas in the vessel than the ideal approach. The main difference is in the carbon dioxide adsorbed. This is because both the binary interaction parameters of carbon dioxide, which is the most strongly adsorbed compound, are higher in magnitude than the interaction parameters of ethane/ethylene, making carbon dioxide equilibrium more sensible to the non-ideal approach. However, total amount of moles in the vessel does not change significantly because carbon dioxide is present in small amount in the feeding mixture.

Table 10: comparison of the amount of moles between ideal and non-ideal compressor after adsorption at 101.325 kPa and 298 K for 1 kg of zeolite 13X.

	Carbon Dioxide	Ethylene	Ethane	Total
Ideal case				
Bulk gas phase	0.002	0.007	0.038	0.048
Adsorbed phase	0.459	0.041	2.183	2.683
Total	0.461	0.048	2.221	2.731
Non-ideal case				
Bulk gas phase	0.002	0.007	0.038	0.047
Adsorbed phase	0.756	0.045	2.079	2.880
Total	0.758	0.052	2.117	2.927

The excess part of the total adsorbed amount (eq. (20)) makes the compressor performance also dependent of the excess thermodynamic potentials which are inverse functions of temperature. This results in a decrease of the excess adsorbed amount with increasing temperatures. Thus, the non-ideal approach introduces a higher sensitivity of equilibrium with temperature. This is illustrated in Fig. 7, where in the non-ideal compressor the release of gas from the adsorbed phase to the bulk gas phase is larger than the ideal compressor, resulting eventually in higher equilibrium pressures.

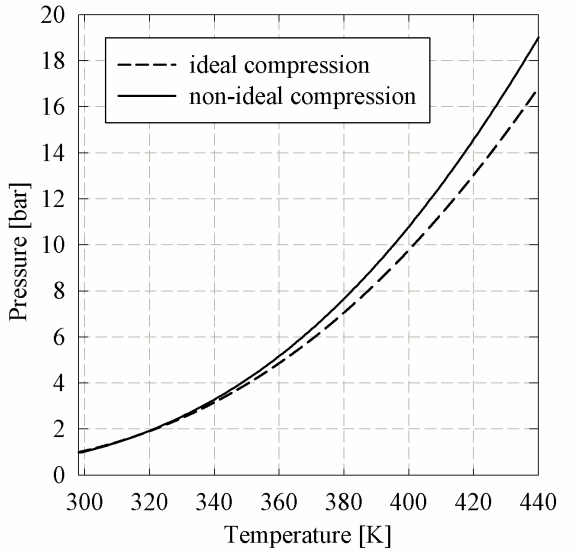

Figure 7: Compression of a gas mixture of Carbon Dioxide/Ethylene/Ethane with 1 kg of zeolite 13X and (0.05,0.15,0.80) feed composition, adsorbed at 101.325 kPa, 298 K. Pressure profile against heating temperature in the ideal (dashed line) and non-ideal (solid line) cases.

In Fig.8, the change in the activity coefficients over temperature promotes increasingly higher pressures. Among the three components, carbon dioxide shows the steepest trend, spanning from 0.55 at 298 K to 0.92 at 440 K. Fugacity coefficients vary in smaller proportion. In this case ethane has the larger variation ranging between 0.992 at 298 K and 0.96 at 340 K.

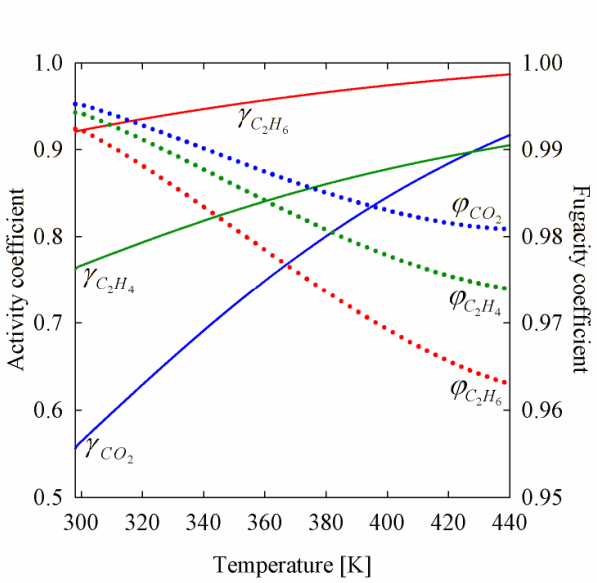

Figure 8: Compression of a gas mixture of Carbon Dioxide/Ethylene/Ethane with 1 kg of zeolite 13X and (0.05, 0.15, 0.80) feed composition, adsorbed at 101.325 kPa, 298 K. Activity and fugacity coefficients profiles against heating temperature.

Compositions in bulk gas phase and adsorbed phase are illustrated in Fig. 9, where adsorbed phase compositions keep essentially constant throughout the heating range, while bulk gas phase compositions visibly change. Also a significant difference is observed in the adsorbed phase compositions of carbon dioxide and ethane between ideal and non-ideal approach already in the adsorption step. The feature of the non-ideal approach of predicting higher pressures depends also on this initial difference.

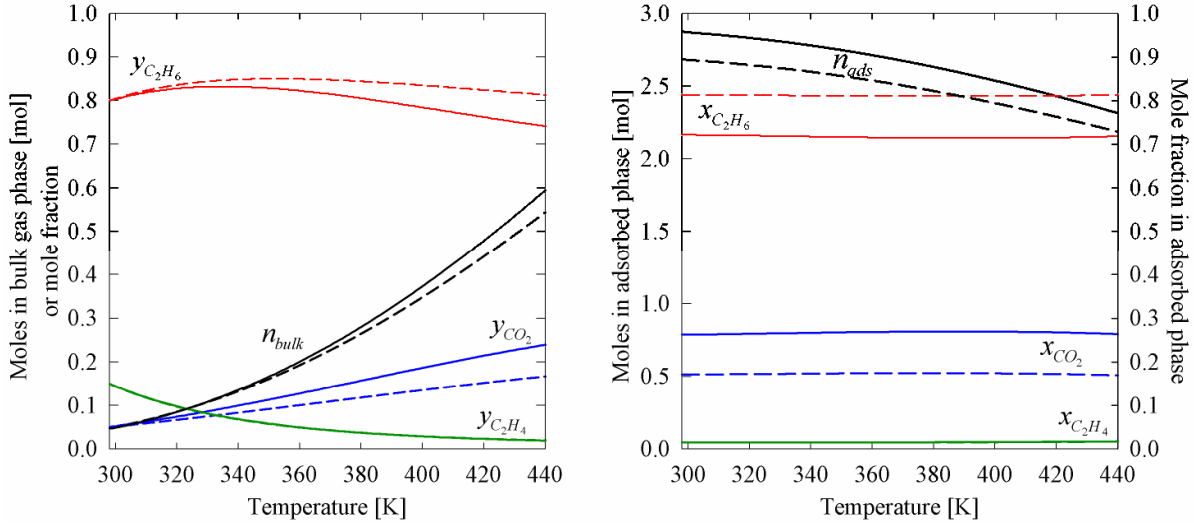

Figure 9: Compression of a gas mixture of Carbon Dioxide/Ethylene/Ethane with 1 kg of zeolite 13X and (0.05,0.15,0.80) feed composition, adsorbed at 101.325 kPa, 298 K. Comparison between compositions, bulk gas phase amount and adsorbed amount against heating temperature in the ideal (dashed line) and non-ideal (solid line) cases.

Fig. 9 shows also that in the bulk gas phase, at temperatures <320 K (<2 bar), the ideal and non-ideal approaches provide the same results, while in the adsorbed phase the two approaches result in significant discrepancies already at low pressure. This is due to non-idealities in the adsorbed phase.

Energy consumption for the two cases is depicted in Fig. 10, where the difference in sensible energy is negligible because it is dominated by the adsorption material heat capacity more than by the adsorbed amount. A difference between ideal and non-ideal desorption heat can be observed already at temperatures >320 K. This difference increases up to 10.5 kJ at 440 K. This results in a lower total energy consumption for the non-ideal compression than ideal compression.

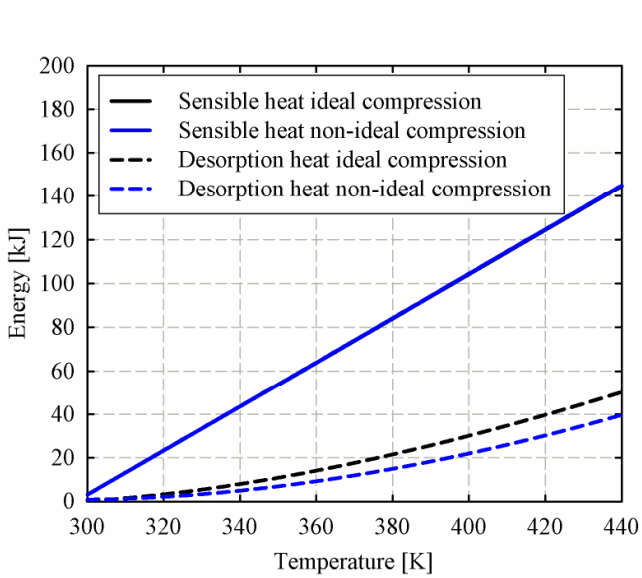

Figure 10: Evolution of sensible and desorption heat at different heating temperatures for 1 kg of zeolite 13X compressing a stream of Nitrogen, Oxygen, Carbon Dioxide. Comparison between ideal and non-ideal compression.

Desorption heat is dominated by the pure component molar integral enthalpies (Δh_i^0) which are similar for the ideal and non-ideal approaches. The second major contribution to the desorption heat consists of the term $RT^2\,(\partial \ln\gamma_i/\partial T)_{\psi,x}$ which is negligible for all gases except that ethane. This builds the difference between ideal compressor and non-ideal compressor in terms of energy consumption. These results show that considerations based on ideal adsorbed solution theory lead to conservative assessment of the compressor performance, with lower pressure generated at higher energy consumption.

5. Conclusion and outlook

Adsorption compressor is an emerging technology which is currently under development for the next long term Mars and lunar missions. Thermodynamics of this system is based on the solution of the isochoric-isothermal flash problem for bulk gas/adsorbed phases. A system composed by Rachford-Rice equation and additional equations embedding the iso-reduced grand potential condition enables the determination of the compressed state. The flash problem has been solved in both cases respectively for two ternary mixtures and validated through its thermodynamic consistency testing the presence of the common tangent plane to the Gibbs energy of mixing at the equilibrium compositions. In this way the applicability of the Rachford-Rice equation is extended to the adsorbed solution theory. This procedure has been applied for the characterisation of one zeolite 13X compressor working ideally with a Nitrogen/Oxygen/Carbon Dioxide gas mixture and non-ideally with a Carbon Dioxide/Ethylene/Ethane mixture. In the latter non-ideal mixture, calculations based on ideal approach proved to be more conservative compared to the non-ideal compressor performance. The application of the proposed thermodynamic framework is at the basis of adsorption compressor performance calculation. The precise design of the single unit and of multi-compressor systems [44] can be reached by embedding the described approach of the equilibrium in the wider dynamic description of the compressor. This impacts directly on the development of sustainable systems that capture, compress and concentrate gases in extremely dilute conditions such as planetary and extra-planetary systems for greenhouse gases removal and compression [45, 46].

Acknowledgements

The research leading to these results has received funding from the European Union Seventh Framework Programme (FP7/2007-2013) under grant agreement n°630863.

Nomenclature

$c_{p,ads}$	Specific heat capacity of the adsorben material [kJ kg^{-1} K^{-1}]
$c_{p,i}$	Specific heat capacity of component i [kJ mol^{-1} K^{-1}]
ex	Excess contribution to the total number of adsorbed moles [kg mol^{-1}]
F	Total number of moles in the feed [mol]

$f_{i,ads}$ Fugacity of pure component i at the system temperature and pressure [kPa]
G Total number of moles in the bulk gas phase [mol]
g_{ex} Excess Gibbs energy [kJ mol^{-1}]
k_i Equilibrium constant of component i
m_{ads} Mass of adsorbent [kg]
N Total number of moles in the adsorbed phase [mol]
NC Number of components participating in the adsorption
n_i Specific amount adsorbed of component i [mol kg^{-1}]. It is calculated directly from adsorption isotherm using either P_i^0 (ideal adsorbed phase) or adsorbed phase fugacity $f_{i,ads}$ (non-ideal adsorbed phase).
$n_{i,ads}$ Amount of adsorbed moles of component i [mol] in adsorbed phase phase;
$n_{i,bulk}$ Amount of adsorbed moles of component i [mol] in bulk gas phase;
P_{bulk} Pressure of the mixture in the bulk gas phase [kPa]
P_i^0 Bulk pressure of the component i at a given reduced grand potential ψ_i [kPa]
R Universal gas constant [kJ mol^{-1} K^{-1}]
T Equilibrium temperature [K]
T_{ads} Temperature of the adsorption bed during adsorption [K]
$T_{heating}$ Temperature of the bed after heating [K]
V_{void} Volume occupied by the bulk gas phase (dead volume) [m^3]
x_i Molar fraction of the component i in the adsorbed phase
y_i Molar fraction of the component i in the bulk gas phase
z_i Molar fraction of the component i in the feed
Z Compressibility factor
ΔH_{ads} Enthalpy for adsorption or desorption [kJ];
ΔH_{sens} Sensible thermal energy and its bulk gas and adsorbed phases [kJ] ;
$\Delta \bar{h}_i$ Differential enthalpy of adsorption [kJ mol^{-1}] for component i in the mixture;
$\Delta \bar{h}_i^0$ Differential enthalpy of adsorption [kJ mol^{-1}] for pure component i;
Δh_i^0 Integral enthalpy of adsorption [kJ mol^{-1}] for pure component i;

Greek letters

γ_i Activity coefficient of component i
ε_b Bed porosity
ε_p Particle porosity
ρ_b Bed bulk density [kg m^{-3}]
$\varphi_{i,bulk}$ Fugacity coefficient of component i in the bulk gas phase
ψ_{eq} Reduced grand potential at equilibrium [mol kg^{-1}]
ψ_i Reduced grand potential of component i [mol kg^{-1}]
Ω Grand potential for adsorption [J kg^{-1}]

References

[1] N. Augustine, J. Ling, P. Xiao, P.A. Webley, Y. Zhai, CO_2 Capture by Temperature Swing Adsorption: Use of Hot CO_2-Rich Gas for Regeneration. Industrial Engineering Chemistry Research 55 (2016) 703-713.

[2] G. Maggio, L.G. Gordeeva, A. Freni, Yu.I. Aristov, G. Santori, F. Polonara, G. Restuccia, Simulation of a solid sorption ice-maker based on the novel composite sorbent "lithium chloride in silica gel pores". Applied Thermal Engineering 29 (2009) 1714-1720.

[3] J.C. Atuonwu, X. Jin, G. van Straten, H.C. van Deventer Antonius, J.B. van Boxtel, Reducing energy consumption in food drying: Opportunities in desiccant adsorption and other dehumidification strategies. Procedia Food Science 1 (2011) 1799-1805.

[4] L. Bonaccorsi, P. Bruzzaniti, L. Calabrese, A. Freni, E. Proverbio, G. Restuccia, Synthesis of SAPO-34 on graphite foams for adsorber heat exchangers. Applied Thermal Engineering 61 (2013) 848-852.

[5] A. Freni, L. Bonaccorsi, L. Calabrese, A. Caprì, A. Frazzica, A. Sapienza, SAPO-34 coated adsorbent heat exchanger for adsorption chillers. Applied Thermal Engineering 82 (2015) 1-7.

[6] Y.Y. Li, S.P. Perera, B.D. Crittenden, J. Bridgwater, The effect of the binder on the manufacture of a 5A zeolite monolith. Powder Technology 116 (2001) 85-96.

[7] G. Li, R. Singh, D. Li, C. Zhao, L. Liu, P.A. Webley, Synthesis of biomorphic zeolite honeycomb monoliths with 16000 cells per square inch. Journal of Materials Chemistry 19 (2009) 8372-8377.

[8] R.E. Critoph, Y. Zhong, Review of trends in solid sorption refrigeration and heat pumping technology. Proceedings of the Institution of Mechanical Engineers 219 (2005) 285-300.

[9] G. Santori,S. Santamaria, A. Sapienza, S. Brandani, A. Freni, A., A stand-alone solar adsorption refrigerator for humanitarian aid. Solar Energy 100 (2014) 172-178.

[10] G. Santori, A. Sapienza, A. Freni, A dynamic multi-level model for adsorptive solar cooling. Renewable Energy 43 (2012) 301-312.

[11] G. Santori, A. Frazzica, A. Freni, M. Galieni, L. Bonaccorsi, F. Polonara, G. Restuccia, Optimization and testing on an adsorption dishwasher. Energy 50 (2013) 170-176.

[12] J.W. Wu, M.J. Biggs, P. Pendleton, A. Badalyan, E.J. Hu, Experimental implementation and validation of thermodynamic cycles of adsorption-based desalination. Applied Energy 98 (2012) 190-197.

[13] L. Joss, M. Gazzani, M. Hefti, D. Marx, M. Mazzotti, Temperature Swing Adsorption for the Recovery of the Heavy Component: An Equilibrium-Based Shortcut Model. Industrial and Engineering Chemistry Research 54 (2015) 3027-3038.

[14] E.M. Mattox, J.C. Knox, D.M. Bardot, Carbon dioxide removal system for closed loop atmosphere revitalization, candidate sorbents screening and test results. Acta Astronautica 86 (2013) 39-46.

[15] R.J. Kay, D. El Sherif, Carbon Dioxide Removal Assembly Performance Comparison. SAE Technical paper 2009-01-2431.

[16] L. Mulloth, J. Finn, A Solid-State Compressor for Integration of CO_2 Removal and Reduction Assemblies. SAE Technical Paper 2000-01-2352.

[17] L.M. Mulloth, J.E. Finn, Air quality systems for related enclosed spaces: spacecraft air, in: D. Barceló, A.G. Kostianoy (Eds), The Handbook of Environmental Chemistry, Springer-Verlag, Berlin, 2005, part H, pp. 383-404.

[18] E. Seedhouse, Lunar Outpost. The Challenges of Establishing a Human Settlement on the Moon, Praxis Publishing Ltd, Chichester, UK, 2009.

[19] H.J. Strumpf, C.Y. Chin, G.R. Lester, S.T. Homeyer, Sabatier Carbon Dioxide Reduction System for Long-Duration Manned Space Application, SAE Technical Paper 911541.

[20] J.C. Knox, M. Campbell, L.A. Miller, L. Mulloth, M. Varghese, B. Luna, Integrated Test and Evaluation of a 4-Bed Molecular Sieve, Temperature Swing Adsorption Compressor, and Sabatier Engineering Development Unit, SAE Technical Paper 2006-01-2271

[21] R.P. Hoover, P.C. Wankat, Gas compression using temperature swing adsorption. Separation Science and Technology 37 (2002) 3187-3199.

[22] J. R. Moate, Temperature swing adsorption compression and membrane separations, PhD thesis, Vanderbilt University, 2009.

[23] J.R. Moate, M.D. LeVan, Temperature swing adsorption compression: Effects of nonuniform heating on bed efficiency. Applied Thermal Engineering 30 (2010) 658-663.

[24] V.F. Cabral, M. Castier, F.W. Tavares, Thermodynamic equilibrium in systems with multiple adsorbed and bulk phases. Chemical Engineering Science 60 (2005) 1773-1782.

[25] A.L. Myers, J.M. Prausnitz, Thermodynamics of mixed-gas adsorption. AIChE Journal 11 (1965) 121-127.

[26] G. Santori, M. Luberti, S. Brandani, Common tangent plane in mixed-gas adsorption. Fluid Phase Equilibria 392 (2015) 49-55.

[27] H.H. Rachford Jr., J.D. Rice, Procedure for Use of Electronic Digital Computers in Calculating Flash Vaporization Hydrocarbon Equilibrium. Journal of Petroleum Technology 195 (1952) 327-328.

[28] O. Talu, A. Myers, Rigorous Thermodynamic Treatment of Gas Adsorption. AIChE Journal 34 (1988) 1887-1893.

[29] F.V.S. Lopes, C.A. Grande, A.M. Ribeiro, J.M. Loureiro,O. Evaggelos, V. Nikolakis, A.E. Rodrigues. Adsorption of H_2, CO_2, CH_4, CO, N_2 and H_2O in Activated Carbon and Zeolite for Hydrogen Production. Separation Science and Technology 44 (2009) 1045-1073.

[30] S.K. Henninger, M. Schicktanz, P.P.C. Hugenell, H. Sievers, H.M. Henning, Evaluation of methanol adsorption on activated carbons for thermally driven chillers part I: Thermophysical characterisation. International Journal of Refrigeration 35 (2012) 543-553.

[31] P. Xiao, J. Zhang, P. Webley, G. Li, R. Singh, R. Todd, Capture of CO_2 from flue gas streams with zeolite 13X by vacuum-pressure swing adsorption. Adsorption 14 (2008) 575-582.

[32] H. Verelst, G.V. Baron, Adsorption of oxygen, nitrogen, and argon on 5A molecular sieve. Journal of Chemical and Engineering Data 30 (1985) 66-70.

[33] O. Talu, I. Zwiebel, Multicomponent Adsorption Equilibria of Nonideal Mixtures. AlChE Journal 32 (1986) 1263-1276.

[34] F. Dreisbach, R. Staudt, J.U. Keller, High Pressure Adsorption Data of Methane, Nitrogen, Carbon Dioxide and their Binary and Ternary Mixtures on Activated Carbon. Adsorption 5 (1999) 215-227.

[35] S. Gamba, G.S. Soave, L.A. Pellegrini, Use of normal boiling point correlations for predicting critical parameters of paraffins for vapour-liquid equilibrium calculations with the SRK equation of state. Fluid Phase Equilibria 276 (2009) 133-141.

[36] G. Soave, Equilibrium constants from a modified Redlich-Kwong equation of state. Chemical Engineering Science 27 (1972) 1197-1203.

[37] O. Redlich, J.N.S. Kwong, On the Thermodynamics of Solutions. V. An Equation of State. Fugacities of Gaseous Solutions. Chemical Reviews 44 (1949) 233-244.

[38] F.R. Siperstein, A.L. Myers, Mixed Gas Adsorption. AIChE Journal 47 (2001) 1141-1159.

[39] K.S. Walton, M.D. LeVan, Adsorbed-Phase Heat Capacities: Thermodynamically Consistent Values Determined from Temperature-Dependent Equilibrium Models. Industrial and Engineering Chemistry Research 44 (2005) 178-182.

[40] E.W. Lemmon, M.O. McLinden, M.L. Huber, NIST Standard Reference Database 23, NIST Thermodynamic Properties of Refrigerants and Refrigerant Mixtures Database (REFPROP) Version 9.0. Gaithersburg: National Institute of Standards and Technology (2010)

[41] M. L. Zanota, H. Heymans, F. Gilles, B.L. Su, M. Frère, G. De Weireld, Adsorption Isotherms of Pure Gas and Binary Mixtures of Air Compounds on Faujasite Zeolite Adsorbents: Effect of Compensation Cation. Journal of Chemical and Engineering Data 55 (2010) 448-458.

[42] F.V.S. Lopes, C.A. Grande, A.M. Ribeiro, V.J.P. Vilar, J.M. Loureiro, A.E. Rodrigues, Effect of Ion Exchange on the Adsorption of Steam Methane Reforming Off-Gases on Zeolite 13X. Journal of Chemical and Engineering Data 55 (2010) 184-195.

[43] M.A. Granato, V.D. Martins, J.C. Santos, M. Jorge, A.E. Rodrigues, From molecules to processes: molecular simulations applied to the design of simulated moving bed for ethane/ethylene separation. The Canadian Journal of Chemical Engineering 92 (2014) 148-155.

[44] G. Santori, Open-cycle adsorption compression train, Sorption Friends meeting, Milazzo, Italy, 2015.

[45] M.-C. Ferrari, D. Friedrich, G. Santori, S. Brandani, Design of a small scale air capture system, FOA11: 11th International Symposium on the Fundamentals of Adsorption, Baltimore, MD, United States, 2013.

[46] C. Charalambous, M.-C. Ferrari, S. Brandani, G. Santori, Thermally-driven adsorption, concentration and purification of highly dilute gases, Heat Powered Cycle Conference 2016, Nottingham, UK, 2016.